The International Journal of Advanced Manufacturing Technology (2019) 101:2191–2203
https://doi.org/10.1007/s00170-018-3110-7

ORIGINAL ARTICLE

Investigation and modelling of the cutting forces in turning process of the Ti-6Al-4V and Ti-6Al-7Nb titanium alloys

Sérgio Luiz Moni Ribeiro Filho[1] · Robson Bruno Dutra Pereira[1] · Carlos Henrique Lauro[1] · Lincoln Cardoso Brandão[1]

Received: 17 September 2018 / Accepted: 20 November 2018 / Published online: 28 November 2018

Abstract

The algebraic and statistical models have assumed an essential role to better understand the relationship of the cutting parameters and their interactions in the cutting forces. This work evaluated the effects of cutting speed, feed rate, and depth of cut on the cutting force (Fc) and specific cutting force (k_S) in the turning of the Ti-6Al-4V and Ti-6Al-7Nb titanium alloys. The experimental tests were carried out with two different insert tools under dry conditions. A response surface method was employed for modelling and better understanding the correlation between the cutting forces and the independent parameters. A central composite design was used as experimental planning. The adequacy and significance of the response model were identified using the analysis of variance (ANOVA). The developed RSM models showed a good degree of fit, which indicates that the cutting force models can be effectively used to estimate the responses in the turning of the Ti-6Al-4V and Ti-6Al-7Nb titanium alloys. The lowest force components were found when the depth of cut and feed rate levels are small and cutting speed is high. Furthermore, the depth of cut was the most significant factor influencing the cutting efforts. Finally, k_S values were mainly influenced by chip thickness, while the cutting speed has not affected the k_S data.

Keywords Ti-6Al-4V · Ti-6Al-7Nb · Turning · Response surface method

1 Introduction

The cutting forces in micro and macro machining processes are one of the most descriptive data to determine the performance and the cutting tool lifetime. Besides, the cutting forces are a typical output to characterise the power required for the machining process, the tool wear, and the system stability, affecting, consequently, the economic viability of the operation. In this way, the cutting force can be employed as a critical process response identifying the optimal cutting parameters [1, 27]. Several types of research in the machining area have been developed with the purpose of measuring cutting forces in the turning process. Yuan et al. [1] stated that the precise estimation of the cutting forces in the different system parameters is fundamental to economically integrate and optimise the quality of the machining process with the extension of the tool life. The authors postulated a new model using a hybrid approach to predict the cutting force of the micro end-milling accurately.

Orra and Choudhury [2] presented a mechanistic cutting force model based on three-dimensional cutting operations. The force model has been proposed for predicting cutting forces during the chip formation with the worn tool. The approach machining parameters ed was achieved an accurate prediction and a good agreement with experimental results. Heydarzadeh et al. [3] have developed a model to accurately estimate the disturbing forces along the micro-milling process using a neural network and Kalman filter. It was observed that the friction and force ripples are the main disturbing forces that affected the micro-milling forces estimations.

The modelling of the cutting forces involved in the cutting processes is extremely complex, presents a nonlinear feature, and can be composed by multiple parameters and responses.

✉ Lincoln Cardoso Brandão
lincoln@ufsj.edu.br

Sérgio Luiz Moni Ribeiro Filho
sergiolmrf@gmail.com

Robson Bruno Dutra Pereira
robsondutra@ufsj.edu.br

Carlos Henrique Lauro
caiquelauro@gmail.com

[1] Department of Mechanical Engineering, Centre for Innovation in Sustainable Manufacturing, Federal University of São João del-Rei, Praça Frei Orlando, 170, centro, São João del Rei 36.307-352, Brazil

Analytic models, mechanistic conceptions, and hybrid approaches are extensively applied to modelling the cutting forces [4]. A variety of studies have been conducted on the development of cutting force models to optimise the machining parameters and improve the stability in the turning process. Hanief et al. [5] developed a regression model and artificial neural network (ANN) to predict the cutting forces during the turning operation of red brass (C23000) using high-speed steel (HSS) tool. A statistical approach was found capable of estimating the cutting forces with satisfactory accuracy, although the ANN concept showed higher accuracy than the regression model in the study.

Cascón and Sarasua [6] investigated a mechanistic model integrated into a CAM software to approximately estimate the orthogonal turning forces, torque, and power consumption along the whole tool path. This study shows that the mechanical models, despite the limited accuracy, can predict the cutting forces during the turning operation, and consequently, adapt cutting parameters, and detect the critical state of the tool. Dorlin et al. [7] analysed the influence of the geometrical modelling of the convex contact radius of the tool-workpiece interface in the cutting forces of the cylindrical and face turning of Ti-6Al-4V titanium alloy. A significant effect of the contact radius was highlighted by the increase of the cutting forces with the rise of the radius. Furthermore, the tool wear intensifies the contact radius effect on the cutting forces.

During recent years, the characteristics of the cutting forces have been widely investigated in various materials, in special, the titanium and their alloys. In general, titanium alloys are used in all aspects of science, engineering, and medicine Mahapatro [27]). Wyen and Wegener [8] identified the forces acting in the Ti-6Al-4V titanium alloy machining process, and thus, they carried out orthogonal turning experiments with different cutting-edge radii, cutting speed, and feeds. According to the authors, the variation of cutting speed has a significant influence on the turning process, mainly on feed force, because there occurred a non-linear influence and depending on the cutting-edge radius.

Rey et al. [9] examined cutting forces in the orbital drilling of the Ti-6Al-4V. A cutting force model was modelled based on the instantaneous chip thickness to optimise the cutting conditions and the geometry of the cutting tool. Ribeiro Filho et al. [10] analysed the effects of the cutting parameters in the turning of Ti-6Al-4V alloy on the cutting forces and corrosion resistance. A response surface method was established in modelling the turning efforts algebraically. Lauro et al. [11] monitored the cutting forces, specific cutting force, friction coefficient, temperature, and shear plane angle during the micro-cutting of the Ti-6Al-7Nb. Signal processing techniques were conducted to determine the influence of the cutting speed, feed rate, and spindle speed on the behaviour of the biomedical titanium alloy. Lauro et al. [12] investigated the characteristics of sustainable micro-cutting through the ploughing effect on minimum quantity lubrication (MQL) and high-speed machining conditions on the Ti-6Al-7Nb alloy. The cutting forces, the specific cutting force, the shear plane, the friction coefficient, the chip, and the surface quality were examined to verify the feature of the titanium alloy.

The present research aims to model and evaluate the cutting parameters in the turning process to obtain a better understanding of the cutting force (Fc) in different titanium alloys. The experimental tests were performed with two insert tools under dry cutting conditions. A response surface method was used to determine the analytical form of the relationship between the cutting force (Fc) and the input parameters. The specific cutting force was calculated by the Horváth [13] and Kienzle-Vitor models. Cutting speed, feed rate, and depth of cut in the Ti-6Al-4V and Ti-6Al-7Nb titanium alloys were set as the influencing parameters in the central composite design (CCD).

2 Methodology

2.1 Turning tests

The experimental tests were performed in a turning-centre with the maximum spindle speed of 6000 rpm and 22.5 kW of main power. Cylindrical bars of Ti-6Al-4V and Ti-6Al-7Nb Titanium alloy of 14 mm in length and 50 mm in diameter were used as workpieces. Triangle carbide tool with ISO code TCMT 110304 - H13A with 7° of clearance angle, noise radius of 0.4 mm, and cutting-edge length of 11 mm was used in experiments. The H13A grade is an uncoated carbide grade that provides excellent abrasion wear resistance and toughness for turning hardened materials at low speeds. Furthermore, the TCMW 110304–3215 with 7° of clearance angle, noise radius of 0.4 mm, and cutting-edge length of 11 mm was also used. The grade 3215 is carbide tool with CVD coating being wear resistant due to the very hard substrate and higher thickness coating, applied under demanding cutting conditions.

Figure 1 shows a schematic design of workpiece with dimensions and the distance of assembly in turning-centre. As can be seen in Fig. 1, the setup used was an overhang of 15 mm without tailstock to increase the rigidity of the system during the turning process. Each turning test was carried out in the length of 14 mm until the end diameter of 15 mm. The input parameters, cutting speed, depth of cut, feed rate, and the kind of titanium alloy were tested randomly.

2.2 Measurement cutting forces

A piezoelectric dynamometer system Kistler 9272 was employed to measure the cutting forces in turning operation. The dynamometer was connected to a Kistler amplifier 5070, and the sensitivity was evaluated (pC/N) with a loss pass filter

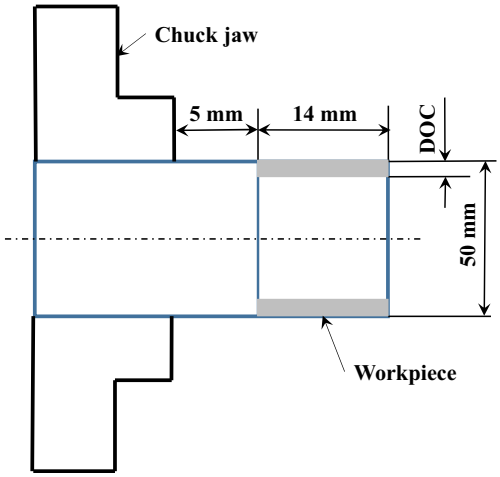

Fig. 1 Detail of workpiece of Ti-6Al-4V and Ti-6Al-7Nb titanium alloys

and an error curve determined in the range from 0 to 100 N. The Fc (cutting force) was recorded using a piezoelectric dynamometer with an acquisition rate of 500 Hz.

2.3 Modelling the cutting forces

The cutting force (Fc) has been defined as a response since each input parameter can be or not influence on cutting force. Thus, a design of experiments based on response surface methodology (RSM) was used to provide random tests without replicates and with the aiming of optimisation the better conditions in the turning process. In the experimental tests, only new tools were used, and one edge per test was used.

2.4 Experimental planning

Turning tests, according to input parameters in Table 1, were carried out randomly based on response surface methodology (RSM). Thus, 20 experimental tests were carried out, namely eight cube points, four centre points in a cube, six axial points, and two centre points in axial. The response surface method provides an approach that facilitates the modelling and examines of the processes with a multivariable feature. In this instance, the RSM approach represents a key factor to identify the optimal condition of the turning parameters to obtain the desired response.

Table 1 Factors and levels of CCD design for each insert carbide tool and titanium alloy

Factors	Symbol	Levels				
		− 1.68	− 1	0	1	1.68
Cutting speed (m/min)	v_c	50	54.8	62.5	70.2	75
Feed rate (mm/rev)	f	0.05	0.089	0.15	0.211	0.25
Depth of cut (mm)	DOC	0.2	0.355	0.6	0.845	1

A central composite design (CCD) was carried out to evaluate the effect of the feed rate, cutting speed and depth of cut on the cutting force (Fc) for each insert carbide tool and titanium alloy. The CCD represents a 2^k factorial design with n_f factorial points, 2^k axial points, and n_C centre points. This planning design does not include all combinations of the experimental factors (k) and their respective levels (n). Therefore, the CCD is very useful to modelling and analyse the effects of the input parameters in the first- and second-order model.

2.5 Definition and calculation of specific cutting force

According to Horváth [13], the Kienzle-Victor model is widely used to calculate the components in machining forces with the focus on cutting force (Fc). It can be considered that the specific cutting force (k_S) depends on cutting section defined by chip dimensions but is well known that the model is based on the theoretical undeformed chip width, b, and chip thickness, h. The (k_S) coefficient can be defined as the cutting force (Fc) in the tangential direction needed to cut a chip area of 1 mm^2 that has a thickness of 1 mm. However, the (k_S) is a coefficient that depends on the material, the material and coating of the tool, and the geometry of the cutting edges. Based on this, there is not a unique database for the coefficient (k_S), because it is necessary calculating the (k_S) coefficient for each couple tool/material by experimental tests [14].

In the turning process, there are two situations to be considered, such as theoretical chip cross-section according to Fig. 2(a) and a true chip cross-section based on Fig. 2(b), mainly in finishing turning process when the depth of cutting is lower or proportional than tip radius of tool and side cutting angle of the tool (κ_r) is 90°.

It can be considered that the main value of specific cutting force (k_S) and the exponent of chip thickness (q) can be determined experimentally. Thus, as defined and studied in several references ([15]; Hertel et al. [24]), the value of the specific cutting force depends on the pair machined material/cutting tool, being true for chip dimensions $b = 1$ mm and $h = 1$ mm. Moreover, according to Grądzka et al. [16] the Kienzle model can predict both nonlinear dependences of cutting force on uncut chip thickness h due to changes of the shear angle.

Figure 2(a), (b) shows a specific situation where the feed rate (f) is identical to value (h) and the depth of cut "DOC" is the same value of (b) because the side cutting angle of the tool (κ_r) is 90°. Thus, the mathematic model proposed in Eqs. (1) and (2) can be written, and its development has been rewritten according to Eq. (3).

$$h = f.\sin.(\mathrm{Kr}) \tag{1}$$

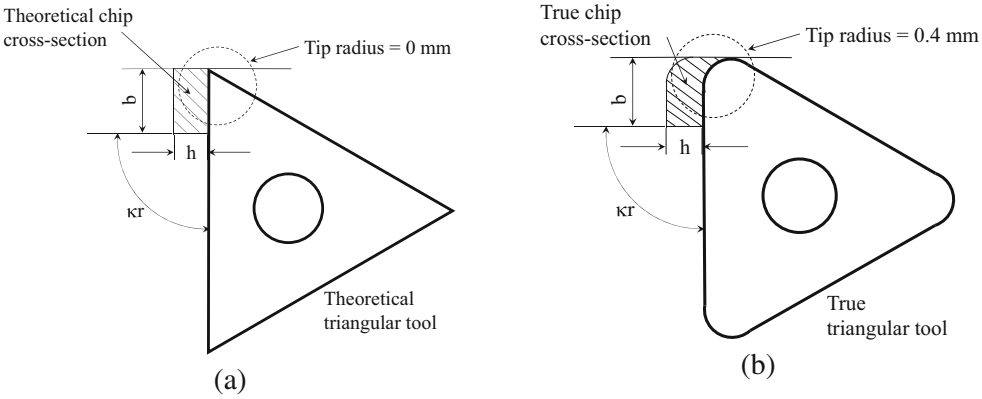

Fig. 2 Theoretical (**a**) and experimental situation (**b**) of cutting section

$$b = \frac{\mathrm{ap}}{\sin.(\mathrm{Kr})} \tag{2}$$

$$F = k\mathrm{S}_{1,0.1}.f^{(1-q)}.\mathrm{DOC} \tag{3}$$

According to Horváth [13], the Kienzle-Victor method can be used in rough turning process because the depth of cut (DOC) is considerably larger than the tip radius of the tool. On the other hand, in the finishing turning operations, a smaller part of the side cutting edge and the whole of the tip radius takes part in chip removal, as can be seen in Fig. 2(b). Based on this, the cutting parameters set in finishing cutting operations, such as side cutting edge angle (κ_r) and the tip radius of the tool (r_ε), are used to determine the cutting length of the edge of the tool (l_{eff}). Based on this theory, chip cross-section can be represented according to Fig. 3 and, given as Eq. (4), follow the model developed by Horváth [13].

The model proposed by Horváth [13] requires the calculation of specific cutting force that can be determined by a piezoelectric dynamometer, which can be written according to Eq. (4) below:

$$\mathrm{Fc} = \frac{F}{A} = \frac{F}{(\mathrm{h_{eq}}).(\mathrm{l_{eff}})} \tag{4}$$

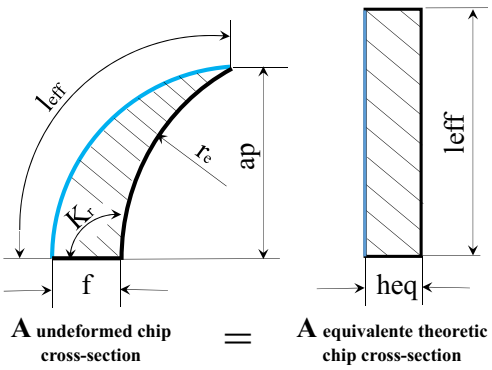

Fig. 3 Chip cross-section for finishing turning process [13, 17]

It can be supported that the obtained (k_{S}) value depends on (h_{eq}) and (l_{eff}). Therefore, it is possibly modelling them with a two-factor regression function as written below:

$$k_s = C.(h_{eq})^q.(l_{eff})^y \tag{5}$$

Based on this, in Eq. (5), the fitting parameter (C) is a positive number, and (q) and (y) are empirically estimated exponents. Thus, if we provide the substitution for h_{eq} = 0.1 mm, the value of $k_{\mathrm{S}(1,0.1)}$ can be written as below:

$$k_{\mathrm{S}(1,0.1)} = C.(0.1)^q \tag{6}$$

Thus, according to Eq. (6), the value of (C) constant, which depends on equivalent chip thickness and the cutting length, for the two titanium alloys, can be calculated according to Eq. (7) below:

$$C = \frac{k_{\mathrm{S}(1,0.1)}}{(0.1)^q} = \frac{k_{\mathrm{S}(1,0.1)}}{(10)^{-q}} = k_{\mathrm{S}(1,0.1)}.(10)^q \tag{7}$$

Finally, the resulting general cutting force (Fc) model and definition of specific cutting force (k_{S}) can be described according to the Eqs. (8) and (9) below:

$$F = k_{\mathrm{s}}.h_{\mathrm{eq}}.l_{\mathrm{eff}} = k_{\mathrm{s}(1,0.1)}.(10)^{\mathrm{q}}.(h_{\mathrm{eq}})^{(1+q)}.(l_{\mathrm{eff}})^{(1+y)} \tag{8}$$

$$k_{\mathrm{s}(1,0.1)} = C.(h_{\mathrm{eq}})^q.(l_{\mathrm{eff}})^y \tag{9}$$

Moreover, it can be considered that in fine turning, the effective edge length (l_{eff}) can be defined based on depth of cut (DOC), feed rate (f), side cutting edge angle (κ_r), and tip radius of the tool (r_ε), as shown in the Eq. (10) below. On the other hand, the (h_{eq}) value also can be calculated according to Eq. (11).

$$l_{\text{eff}} = \frac{(\text{DOC}-r_{\varepsilon.}).\left(1-\cos.\left(k_{\text{r}}\right)\right)}{\sin.(k_{\text{r}})} + r_{\varepsilon}.\left(k_{\text{r}} + \arcsin.\left(\frac{f}{2.r_{\varepsilon}}\right)\right) \quad (10)$$

$$h_{\text{eq}} = \frac{(\text{DOC}).(\text{af})}{l_{\text{eff}}} \quad (11)$$

where

DOC	depth of cut (mm)
f	feed rate (mm/rev)
r_{e}	tip radius (mm)
κ_{r}	side cutting edge (rad)
Fc	cutting force (N)
$k_{1,0.1}$	constant value of main specific cutting force (N/mm^2) (where $h_{\text{eq}} = 0.1$ mm and $l_{\text{eff}} = 1$ mm)
h_{eq}	cutting length of the edge of the tool (mm)
l_{eff}	the cutting length of the edge of the tool (mm)
q and y	constants of the regression Equation (dimensionless)

3 Analysis of results

The RSM design was adopted to help quantifying and better understanding the relationships between cutting force (Fc) and the turning parameters. In general, the RSM approach describes if the surface has an adequate approximation model, and then the analysis will fit the actual process. The response (Y) and the predictor variables can be expressed according to the Taylor series in Eq. (12).

$$y = \beta_0 + \sum_{i=1}^{K}\beta_i x_i + \sum_{i=1}^{k}\beta_{ii}x_i^2 + \sum_{i<j}\sum\beta_{ij}x_i x_j + \varepsilon \quad (12)$$

Tables 2 and 3 shows the significance of the factors in the cutting force (Fc) models for Ti-6Al-7Nb e Ti-6Al-4V. The F-value represents the variance ratio, which is the ratio of variance calculated by the effects of the quadratic average adjusted in each factor by the quadratic average adjusted in error. This situation means that the F-value is a measure of the significance of the model with respect to the variance. On the other hand, the P value specifies the probability that these two parameters, the adjusted MS factor and adjusted MS error, have the same value and the model is appropriate. When the P values in Tables 2 and 3 are less or identical than 0.05 (confidence interval of 95%) indicates that the factors and their interactions have a significant effect on the responses model.

In Tables 2 and 3, the calculated values of P value for the model term was 0.000 for the two titanium alloys in the RSM model. This condition revealed that the terms in the surface model of the Ti-6Al-4V and Ti-6Al-7Nb influence the (Fc) response, at least, and one of the terms has a significant effect. Because P value was 0.000, (P value < 0.005) also means that the model is adequate. The lack of fit is a statistical test that measures the ratio between the lack-of-fit mean square and the error mean square. The values of P of lack of fit higher than 0.05 implies that the lack of fit was non-significant for the response model. Thus, it can be suggested that (Fc) model presents a good degree of fit for the independent variables.

A significant coefficient is the R^2, which explained a proportion of the variability in the observations of the cutting force (Fc). Thus, when the R^2 approaches to 1 (100%), the better the prediction of the actual cutting force in the response model. The quadratic response models that correlate the cutting speed (Vc), feed rate (f), and depth of cut (DOC) are presented as follows:

Ti-6Al-7Nb and tool code H13A:

$$\text{Fc(N)} = -145 + 3.96^{*}\text{vc} + 199^{*}\text{DOC} + 390^{*}\text{f} - 0.0216^{*}\text{vc}^{*}\text{vc} - 77.0^{*}\text{DOC}^{*}\text{DOC} + 1002\,\text{f}^{*}\text{f} - 0.62^{*}\text{Vc}^{*}\text{DOC} - 7.8^{*}\text{vc}^{*}\text{f} + 1658^{*}\text{DOC}^{*}\text{f}$$

Ti-6Al-7Nb and tool code 3215:

$$\text{Fc(N)} = 101 - 3.3^{*}\text{vc} + 15^{*}\text{DOC} + 1259^{*}\text{f} + 0.0330^{*}\text{vc}^{*}\text{vc} + 12.4^{*}\text{DOC}^{*}\text{DOC} - 3005^{*}\text{f}^{*}\text{f} - 0.02^{*}\text{vc}^{*}\text{DOC} - 7.9^{*}\text{vc}^{*}\text{f} + 2159^{*}\text{DOC}^{*}\text{f}$$

Ti-6Al-4V and tool code H13A:

$$\text{Fc(N)} = -36 - 0.35^{*}\text{vc} + 254.4^{*}\text{DOC} + 568^{*}\text{f} + 0.0089^{*}\text{vc}^{*}\text{vc} - 65.2^{*}\text{DOC}^{*}\text{DOC} - 1738^{*}\text{f}^{*}\text{f} - 1.41^{*}\text{vc}^{*}\text{DOC} + 0.07^{*}\text{vc}^{*}\text{f} + 1688^{*}\text{DOC}^{*}\text{f}$$

Ti-6Al-4V and tool code 3215

$$\text{Fc(N)} = 130 - 9.3^{*}\text{vc} + 392^{*}\text{DOC} + 1844^{*}\text{f} + 0.121^{*}\text{vc}^{*}\text{vc} - 57^{*}\text{DOC}^{*}\text{DOC} - 1194^{*}\text{f}^{*}\text{f} - 4.08^{*}\text{vc}^{*}\text{DOC} - 24.6^{*}\text{vc}^{*}\text{f} + 1933^{*}\text{DOC}^{*}\text{f}$$

3.1 Cutting force (fc)

Tables 2 and 3 show the analysis of variance (ANOVA) for cutting force (Fc) quadratic model. The feed rate (f) and depth of cut (DOC) were the individual factors that significantly affected the cutting force (Fc). Analysing the pairwise (two-way) interaction only in the interaction, depth of cutting vs. feed rate, occurred an influence on cutting force (Fc). Besides, the contribution values presented in Tables 2 and 3 indicate the most factor that contributed to the variation of the cutting force (Fc). As can be seen, the depth of cut was the factor most

Table 2 Analysis of variance of the cutting force (Fc) model for Ti-6Al-7Nb

Factors and interactions	Ti-6Al-7Nb					
	Tool code H13A			Tool code 3215		
	F-value	*P* value	Contribution	*F*-value	*P* value	Contribution
Main values						
Linear	238.94	0.000	95.18%	189.88	0.000	92.67%
Vc (m/min)	0.29	0.602	0.04%	0.30	0.597	0.05%
DOC (mm)	378.93	0.000	50.31%	339.67	0.000	55.26%
f (mm/rev)	337.61	0.000	44.83%	229.66	0.000	37.36%
Square model						
Vc vs. Vc	0.10	0.759	0.01%	0.17	0.690	0.05%
DOC vs. DOC	1.33	0.275	0.20%	0.03	0.877	0.02%
vs. *f*	0.88	0.370	0.12%	5.73	0.038	0.93%
Two-way interaction						
Vc vs. DOC	0.05	0.825	0.01%	0.00	0.994	0.00%
Vc vs. *f*	0.51	0.493	0.07%	0.37	0.556	0.06%
DOC vs. *f*	23.27	0.001	3.09%	28.53	0.000	4.64%
Lack-of-fit	2.34	0.186		0.94	0.526	
S	14.5325			17.0841		
R^2	98.67%			98.37%		
R^2 (adj)	97.48%			96.91%		
R^2 (pred)	92.35%			91.46%		

effective to improve the cutting force for the Ti-6Al-4V and Ti-6Al-7Nb titanium alloys.

The 3D response surface plots for the cutting force (Fc) are shown in Figs. 4 and 5. As shown in the surface graphs, the quadratic model fitted revealed a curvilinear profile for all the variations of the cutting parameters. The lowest cutting force (Fc) was obtained when the feed rate and depth of cut levels are low, and the cutting speed is high, independent of the tool and titanium alloy. This feature can be associated to the plastic deformation, shearing stresses, vibration, and thermal effects

Table 3 Analysis of variance of the cutting force (Fc) model for Ti-6Al-4V

Factors and interactions	Ti-6Al-4V					
	Tool code H13A			Tool code 3215		
	F-value	*P* value	Contribution	*F*-value	*P* value	Contribution
Model						
Linear	985.71	0.000	95.90%	86.04	0.000	91.26%
Vc (m/min)	0.08	0.785	0.00%	0.16	0.697	0.06%
DOC (mm)	1842.57	0.000	59.75%	161.79	0.000	57.20%
f (mm/rev)	1114.48	0.000	36.14%	96.17	0.000	34.00%
Square						
Vc vs. Vc	0.07	0.794	0.01%	1.04	0.332	0.43%
DOC vs. DOC	4.00	0.073	0.10%	0.24	0.635	0.07%
f vs. *f*	11.06	0.008	0.36%	0.41	0.534	0.15%
Two-way interaction						
Vc vs. DOC	1.11	0.316	0.04%	0.74	0.411	0.26%
Vc vs. *f*	0.00	0.990	0.00%	1.66	0.227	0.59%
DOC vs. *f*	100.78	0.000	3.27%	10.49	0.009	3.71%
Lack-of-fit	1.02	0.492		4.36	0.066	
S	7.10715			25.2292		
R^2	99.68%			96.46%		
R^2 (adj)	99.38%			93.28%		
R^2 (pred)	98.37%			82.79%		

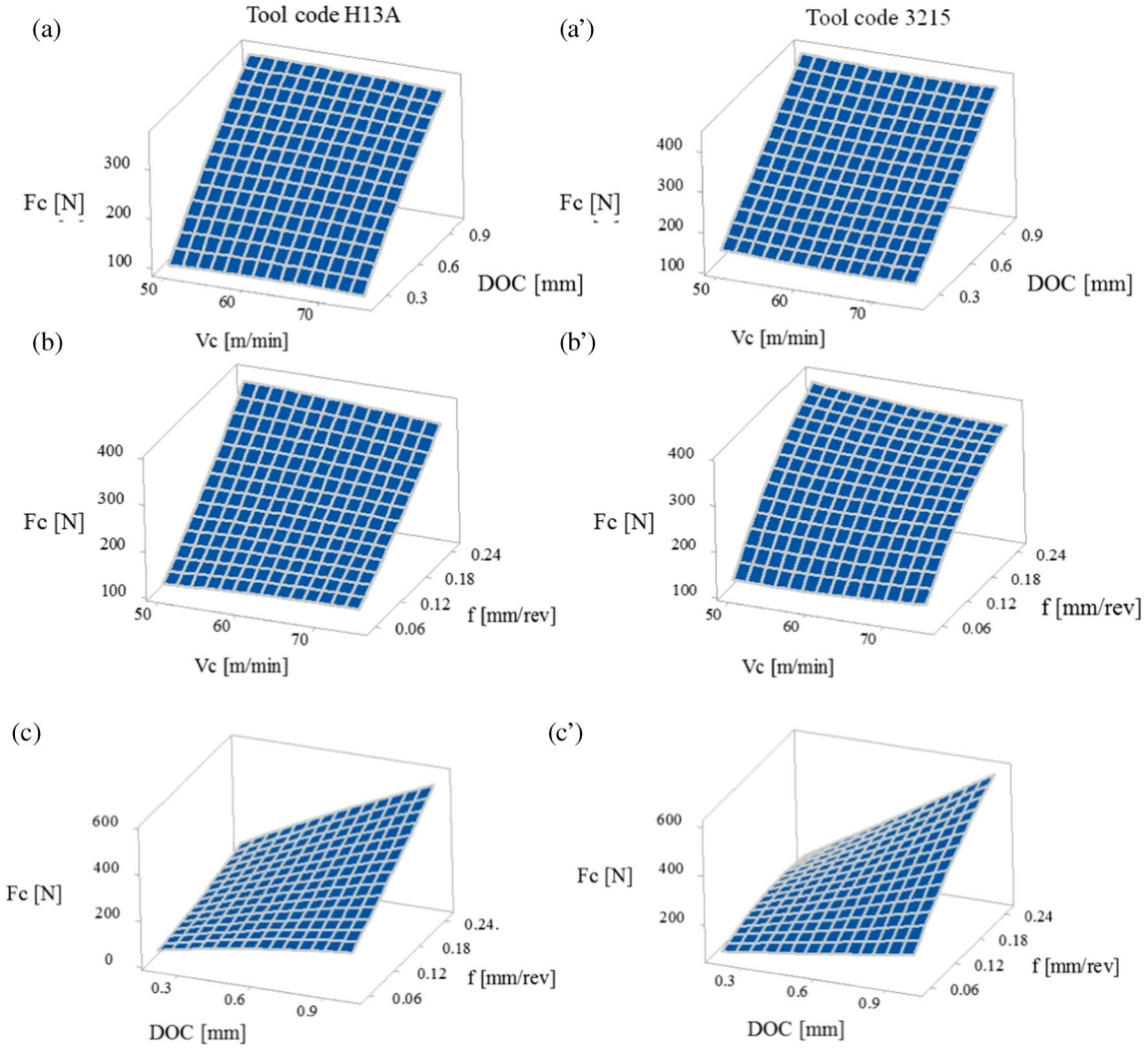

Fig. 4 Surface plot of the cutting force (Fc) in the Ti-6Al-7Nb for the insert tool 13 (**a**–**c**) and code 3215 (**a'**–**c'**)

by the variation in the cutting section that is influenced by the cutting speed (Vc), feed rate (f), and depth of cut (DOC) in the turning process [23, 26].

The main effects and interaction graphs were plotted to identify the effects of the cutting speed (Vc), feed rate (f), and depth of cut (DOC) and their interactions on the cutting force (Fc). Figure 6 exhibits the behaviour of cutting force (Fc) according to the variation of cutting speed, depth of cut, feed rate, tool code, and titanium alloy. It can be noted that cutting force (Fc) tends to increase proportionally to the depth of cut variation and feed rate, observed in Fig. 6(b, c).

The range of values was 119.4 to 391.2 N representing a variation of 228%. The depth of cut and feed rate are responsible to main cutting force because they are a cutting section in the turning process. Thus, the simultaneous increase of only one or both represents a proportional increase in cutting force. However, the cutting force (Fc) based on the feed rate variation was 173.47%, within a range of 134.1 to 366.7, demonstrating that depth of cut has more influence on cutting force (Fc) than feed rate (f), as can be seen in Fig. 6(b) and Tables 2 and 3.

According to Meng et al. [18], all cutting tools used in machining processes tend to deform plastically under the influence of the high compressive stresses and temperatures obtained in machining processes such as turning, milling, and drilling when high cutting speeds and feed rates are used. Thus, the cutting section defined by the depth of cut vs. feed rate can occur in some situations to optimise one pass at a time or when more than one pass is required to remove the total radial dimension the use of the multipass case.

Furthermore, it should be well known that the use of high values for feed rate and depth of cutting can reduce the machining time significantly but will increase the tool wear and depending on the cutting section a plastic deform of the tool can occur. Therefore, the extreme turning condition with the use in the limit of depth of cut and feed rate values should be well thought with views not only of time reduction but also the continuous improvement of quality.

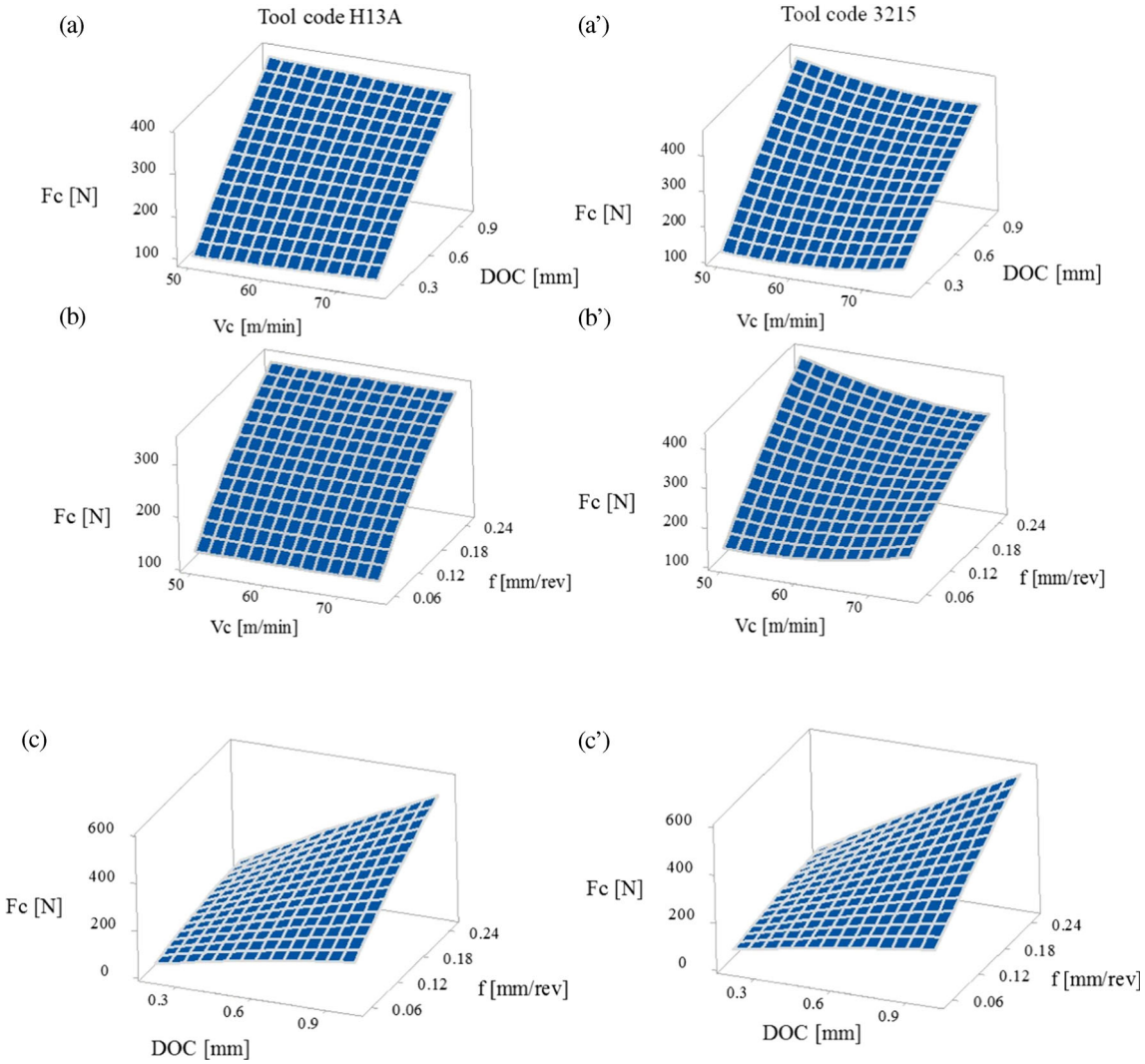

Fig. 5 Surface plot of the cutting force (Fc) in the Ti-6Al-4V for the insert tool 13 (**a**, **b**, and **c**) and code 3215 (**a'**–**c'**)

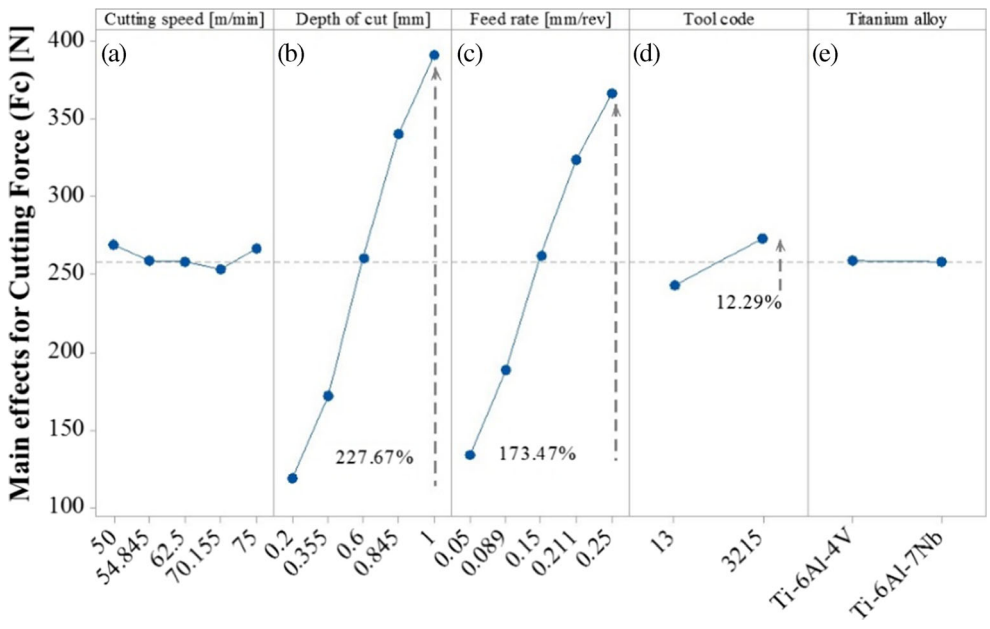

Fig. 6 Main effects for cutting force (Fc)

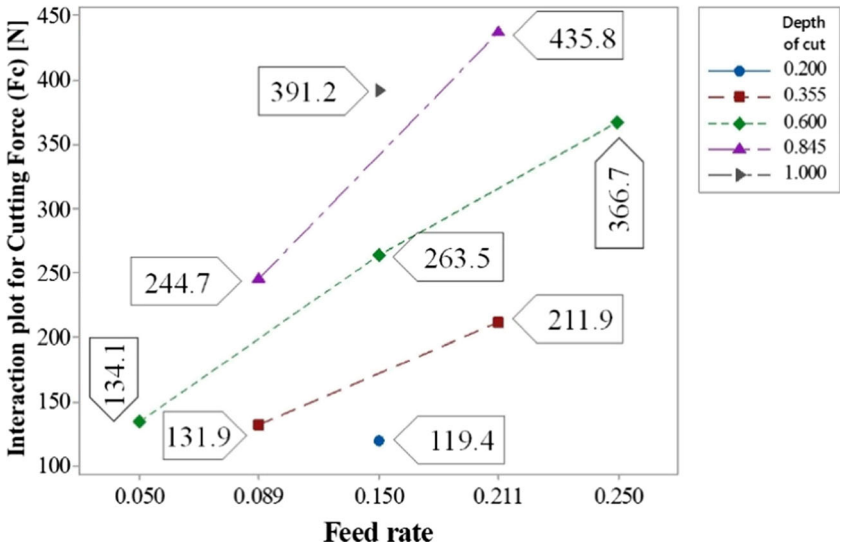

Fig. 7 Interaction for depth of cut (DOC) vs. feed rate (f)

Considering the tool variation influence on cutting force (Fc), as can be seen in Fig. 6(d), it can be noted that the range was similar to surface roughness with a range of 243.3 to 273.3 N and 12% in variation. However, despite lower variation, the kind of tool had an influence on cutting force (Fc) due to the geometry of rake angle that can influence chip formation and temperature generated in turning process as commented before.

Figure 7 shows the interaction effects for depth of cut vs. feed rate for cutting force (Fc). It can be noted that, considering the midpoint of 0.150 mm/rev for feed rate, it occurred a proportional increase of the cutting force (Fc) with a range of

Table 4 Experimental points for Ti-6Al-4V titanium alloy

Titanium alloy	Depth of cut (DOC) (mm)	Feed rate (mm/rev)	h_{eq} (mm)	l_{eff} (mm)	Cutting section (mm)	Cutting speed (m/min)	Cutting force (N)	k_S (N/mm^2)
Ti-6Al-4V	0.6	0.05	0.04	0.85	0.030	70.2	95.70	3190.0
Ti-6Al-4V	0.6	0.05	0.04	0.85	0.030	54.8	114.16	3805.3
Ti-6Al-4V	0.2	0.15	0.06	0.50	0.030	62.5	87.31	2910.3
Ti-6Al-4V	0.355	0.089	0.05	0.63	0.032	70.2	100.16	3170.1
Ti-6Al-4V	0.355	0.089	0.05	0.63	0.032	62.5	85.42	2703.6
Ti-6Al-4V	0.355	0.211	0.11	0.69	0.075	70.2	163.09	2177.3
Ti-6Al-4V	0.355	0.211	0.11	0.69	0.075	54.8	174.14	2324.8
Ti-6Al-4V	0.355	0.211	0.11	0.69	0.075	50.0	164.80	2200.1
Ti-6Al-4V	0.355	0.211	0.11	0.69	0.075	62.5	151.72	2025.5
Ti-6Al-4V	0.845	0.089	0.07	1.12	0.075	62.5	190.84	2537.6
Ti-6Al-4V	0.845	0.089	0.07	1.12	0.075	54.8	223.28	2969.0
Ti-6Al-4V	0.845	0.089	0.07	1.12	0.075	62.5	187.62	2494.8
Ti-6Al-4V	0.6	0.15	0.10	0.90	0.090	70.2	217.94	2421.6
Ti-6Al-4V	0.6	0.15	0.10	0.90	0.090	54.8	207.52	2305.8
Ti-6Al-4V	0.6	0.15	0.10	0.90	0.090	62.5	230.08	2556.4
Ti-6Al-4V	0.6	0.15	0.10	0.90	0.090	50.0	202.07	2245.2
Ti-6Al-4V	0.6	0.15	0.10	0.90	0.090	75.0	221.47	2460.8
Ti-6Al-4V	1	0.15	0.12	1.30	0.150	54.8	335.54	2236.9
Ti-6Al-4V	0.6	0.25	0.16	0.96	0.150	75.0	303.74	2024.9
Ti-6Al-4V	0.6	0.25	0.16	0.96	0.150	62.5	291.17	1941.1
Ti-6Al-4V	0.845	0.211	0.15	1.18	0.178	70.2	429.73	2410.2
Ti-6Al-4V	0.845	0.211	0.15	1.18	0.178	75.0	364.29	2043.2
Ti-6Al-4V	0.845	0.211	0.15	1.18	0.178	62.5	346.59	1943.9

Table 5 Experimental points for Ti-6Al-7Nb titanium alloy

Titanium alloy	Depth of cut (DOC) (mm)	Feed rate (mm/rev)	h_{eq} (mm)	l_{eff} (mm)	Cutting section (mm)	Cutting speed (m/min)	Cutting force (N)	k_S (N/mm^2)
Ti-6Al-7Nb	0.6	0.05	0.04	0.85	0.030	62.5	88.45	2948.3
Ti-6Al-7Nb	0.2	0.15	0.06	0.50	0.030	62.5	87.98	2932.7
Ti-6Al-7Nb	0.2	0.15	0.06	0.50	0.030	54.8	73.80	2460.0
Ti-6Al-7Nb	0.355	0.089	0.05	0.63	0.032	50.0	111.91	3542.0
Ti-6Al-7Nb	0.355	0.089	0.05	0.63	0.032	75.0	90.94	2878.3
Ti-6Al-7Nb	0.355	0.089	0.05	0.63	0.032	70.2	94.57	2993.2
Ti-6Al-7Nb	0.355	0.089	0.05	0.63	0.032	62.5	102.59	3247.0
Ti-6Al-7Nb	0.355	0.211	0.11	0.69	0.075	62.5	161.51	2156.2
Ti-6Al-7Nb	0.355	0.211	0.11	0.69	0.075	54.8	165.75	2212.8
Ti-6Al-7Nb	0.355	0.211	0.11	0.69	0.075	70.2	171.94	2295.4
Ti-6Al-7Nb	0.845	0.089	0.07	1.12	0.075	62.5	195.92	2605.1
Ti-6Al-7Nb	0.845	0.089	0.07	1.12	0.075	70.2	176.86	2351.7
Ti-6Al-7Nb	0.6	0.05	0.04	0.85	0.030	62.5	95.04	3168.0
Ti-6Al-7Nb	0.6	0.15	0.10	0.90	0.090	50.0	215.70	2396.7
Ti-6Al-7Nb	0.6	0.15	0.10	0.90	0.090	54.8	230.46	2560.7
Ti-6Al-7Nb	0.6	0.15	0.10	0.90	0.090	62.5	210.49	2338.8
Ti-6Al-7Nb	0.6	0.15	0.10	0.90	0.090	70.2	212.87	2365.2
Ti-6Al-4V	0.6	0.15	0.10	0.90	0.090	75.0	219.27	2436.3
Ti-6Al-7Nb	1	0.15	0.12	1.30	0.150	62.5	312.34	2082.3
Ti-6Al-7Nb	1	0.15	0.12	1.30	0.150	54.8	346.32	2308.8
Ti-6Al-7Nb	0.6	0.25	0.16	0.96	0.150	62.5	310.53	2070.2
Ti-6Al-7Nb	0.6	0.25	0.16	0.96	0.150	70.2	340.57	2270.5
Ti-6Al-7Nb	0.845	0.211	0.15	1.18	0.178	62.5	391.74	2197.1
Ti-6Al-7Nb	0.845	0.211	0.15	1.18	0.178	70.2	345.38	1937.1

values of 119.4 to 391.2 N. The same situation occurred for the other values of feed rate rising the cutting force (Fc) with feed rate variation when the depth value was set. However, considering the intermediate depth of cut values (0.355, 0.600, and 0.845 mm), the graphics have a linear but non-parallel behaviour.

This situation demonstrated that the non-parallelism in the graphs explains the interaction between feed rate and depth of cut input factors. Thus, it can be stated that the simultaneous variation of feed rate and depth of cut provides an increase in cutting force (Fc), but this behaviour occurs without a proportionality between the input parameters. Thus, it can be considered that cutting force (Fc) was influenced simultaneously by the two parameters of input, feed rate, and depth of cut increasing with the variation of both, though similar values can be obtained, as occurred for example in the range of feed rate of 0.050 and 0.089 mm/rev when depths of cut of 0.355 and 0.600 mm were simultaneously used.

Furthermore, it can be considered that even though the same cutting force (Fc) was produced in this range, between 131.9 and 134.1 N, because the cut sections were very close. The results found in this work are according to Boujelbene [19] that studied the tangential cutting force of titanium alloy Ti-6Al-4V. Although the study was focused on the orthogonal cut, the results demonstrated that the smallest value of the tangential turning force was registered when the highest value of the cutting speed and with the low value of the feed rate was used.

The study carried out by Khan et al. [20] showed the same behaviour in the turning of titanium alloy. According to the authors, the low feed rate was responsible for low cutting forces and temperature, but on the other hand, the high feed was accounted for low chip reduction coefficient. However, it is necessary that a model defines the exact point for feed rate, cutting speed, and depth of cut considering the optimisation process. Mia et al. [21] used a neural network compared to the RSM model to provide optimisation in the turning process. The authors support that the RSM model of cutting force revealed better accuracy with untrained data compared to the ANN models.

Several studies have been carried out in the Ti-6Al-4V alloy aiming to define the exact point for input parameters in turning, milling, and drilling processes to find better surface roughness and lower cutting force values. However, more studies in Ti-6Al-7Nb alloy need to be performed to determine if both alloys have similar behaviour. In this work, the

Table 6 Analysis of variance for cutting force (Fc)

Source			Cutting force (Fc)	
			F-value	*P* value
Main values				
Vc [m/min]			0.84	0.364
DOC [mm]			1463.04	0.000
f [mm/rev]			997.78	0.000
Titanium alloy			0.02	0.880
Tool code			70.01	0.000
Square model				
Vc vs. Vc			0.88	0.352
DOC vs. DOC			1.61	0.209
f vs. *f*			4.40	0.040
Two-way interaction				
Vc vs. DOC			1.04	0.313
Vc vs. *f*			2.76	0.102
Vc vs. titanium alloy			0.02	0.875
Vc vs. tool code			0.09	0.764
DOC vs. *f*			98.60	0.000
DOC vs. titanium alloy			0.78	0.381
DOC vs. tool code			2.23	0.140
f vs. titanium alloy			1.66	0.202
f vs. tool code			0.00	0.950
Titanium alloy vs. tool code			0.46	0.499
Cutting force (Fc) adjust	*S*	R^2	R^2 (Adj)	R^2 (prev.)
Value	15.9967	97.75%	97.08%	95.78%

behaviour of surface roughness and cutting force (Fc) showed a great similarity for both alloys being possible to affirm that it is possible to produce the same surface quality using the same input parameters. Considering the cutting force, the best choice will depend only on the machine power and the use of high depth of cutting values will contribute to reducing the machining time.

3.2 Specific cutting force

The results of experiments shown in Tables 4 and 5 embrace the technological range of fine turning for the feed rate of 0.05–0.25 mm/rev, depth of cut of 0.20–1.0 mm, and cutting speed of 50–75 m/min. In some situations, the experiments were performed with the depth of cut DOC = 0.20 mm that corresponds to DOC < r_ε. However, for the highest value of the depth of cut of 1.0 mm, it was considered that a small section of the side cutting edge also contributes to chip removal. According to Horváth [13], several researchers have reported that cutting speed has a negligible effect on the specific cutting force, but in this work, several cutting speeds were considered not only to verify the cutting speed influence in specific cutting force.

The results for cutting force (Fc) and specific cutting force (k_S) for two titanium alloys tested are shown in Tables 4 and 5. Furthermore, the data in Tables 4 and 5 consider the global values for the two tools tested (TCMT 110304-H13A and TCMW 110304-3215), because the interaction for titanium alloy vs. tool code was considered despicable for cutting force (Fc), as can be seen in Table 6.

As observed in Tables 4 and 5, the approximate values for l_{eff} = 0.90 mm and h_{eq} = 0.1 mm generating a cutting section of 0.09 mm^2, the set of experiments was made so that measurement point determines the values nearest of ($k_{S(1,0.1)}$). It can be occurred because the experimental values were defined according to response surface methodology and subsequently calculated the values of Tables 3 and 4.

As stated in the literature, the cutting speed did not influence the values of (k_S) since the mean value for (k_S) was 2398 N/mm^2 (range of 2245.2–2556.4 N/mm^2) for Ti-6Al-4V titanium alloy and 2419 N/mm^2 (range of 2338.8–2560.7 N/mm^2) for Ti-6Al-7Nb titanium alloy. Furthermore, the standard deviation was 123.94 N/mm^2 and 86.88 N/mm^2, respectively, which corresponds to a 5% and 4% of the variation, being in this way an acceptable variation. Thus, it is

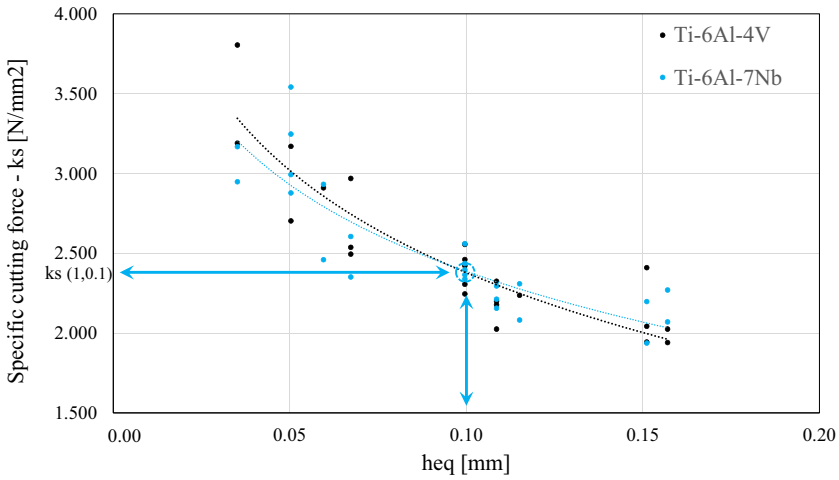

Fig. 8 Specific cutting force as a function of (h_{eq}) for Ti-Al-4V and Ti-Al-7Nb titanium alloy

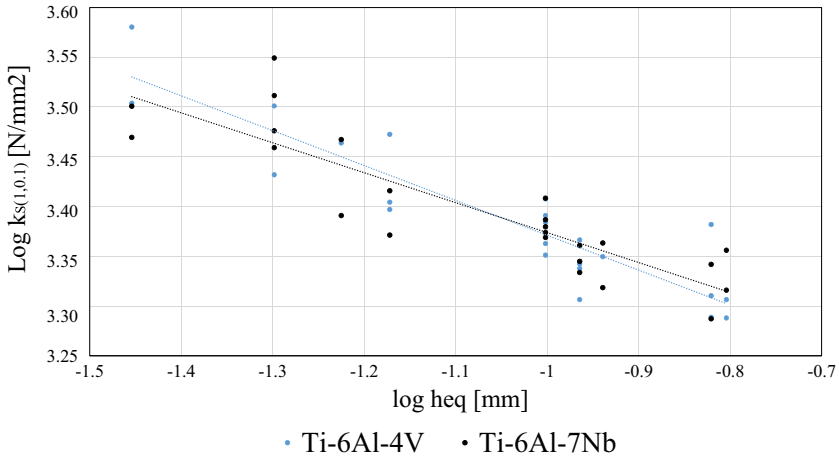

Fig. 9 Specific cutting force as a function of the chip thickness (h_{eq}) on a logarithmic scale graphic

easy to see the possibility to define that the (k_S) value is fulfilled for the pair of values feed rate of 0.15 mm/rev and the depth of cut of 0.6 mm. Figure 8 shows the specific cutting force variation based on cutting length of the edge of the tool (h_{eq}).

It can be supported that the specific cutting force depends on the chip thickness as can be seen in Fig. 4. Thus, according to Kienzle and Victor [15] model, the main value of the specific cutting force can be calculated according to Eq. (6), where $b = 1$ mm, $h_{eq} = 1$ mm, and cutting area = 1 mm^2. The value of (q), in Eq. (6), corresponds to the tangent value of the slope of the line plotted in Fig. 9. The R^2 adjust for two models in Fig. 9 were 0.83 and 0.76 for Ti-6Al-4V and Ti-6Al-7Nb, respectively, which represents an excellent adjust because the values were upper than 0.7 (70%).

Table 7 shows the results for (q), (C), and (y) values for two titanium alloys. Considering the specific cutting force (k_S) and taking the appropriate values from Eq. (7) with the specific cutting force and (q) constant value calculated experimentally, it is possibly defining the (C) value.

The values for (k_S) and the remaining constants show a small difference between the two titanium alloys tested. The difference between the two alloys is the vanadium and niobium composition because the rest of the composition of the two alloys is close because there are 6% aluminium and the titanium correspond to the alloy balance with a difference of 3%.

It can be considered that the main difference between Ti-6AL-4V and Ti-6Al-7Nb alloys is a solid-solution strengthening, the structure-refining strengthening provided by the refined two-phase structure and the difference in the microstructure between the two alloys; however, the strength of Ti-6Al-7Nb alloy is little less than that of Ti-6AL-4V [22]. Thus, the microstructure can provide different shear strengths in the two alloys which are reflected in the calculated specific cutting force (k_S) value. This difference is small due to the used aluminium in the two alloys showing similar values in the perceptual composition.

Table 7 The constant values of the specific cutting force according to the model Eq. (5)

Constant values	Ti-6Al-4V	Ti-6Al-7Nb
$k_{S(1,0.1)}$	2398 N/mm^2	2419 N/mm^2
C	1070.41	1210.14
q	− 0.3503	− 0.3008

4 Conclusions

This study evaluated the turning process in different titanium alloys under dry condition. Cutting forces were investigated in experimental tests, and the results were discussed. The results can be summarised as follows:

- The RSM approach in face central composite design showed that were beneficial and suitable to save several experimentations required once that the R^2 coefficients of the quadratic models were close to 1 (100%). This feature was especially observed in cutting force (Fc) analysis for the Ti-6Al-4V, and Ti-6Al-7Nb for both insert tools.
- The analysis of variance (ANOVA) revealed that the depth of cut was the most relevant factor on the cutting force (Fc). Besides, the result of the ANOVA has demonstrated that the mathematical models fit values of the cutting force.
- The optimum process condition was achieved to be cutting speed of 70.155 m/min, depth of cut of 0.2 mm, and feed rate of 0.05 mm/rev with the tool code H13A for both Ti-6Al-4V and Ti-6al-7Nb titanium alloys.
- The specific cutting force was estimated in function of the mathematical formula of the cutting model. The formula proved a good degree of fit for both titanium alloys.
- The (k_S) values were mainly affected by the equivalent chip thickness. Besides, it is also verified the cutting speed

to not influence the output of (k_S) for both materials used in this work.

Funding information The authors were financially supported by the CNPq - National Research Council and the FAPEMIG - Foundation of Support to the Research of the Minas Gerais State in the Project APQ-01987/14.

References

1. Yuan Y, Jing X, Ehmann KF, Cao J, Li H, Zhang D (2018) Modeling of cutting forces in micro end-milling. J Manuf Process 31:844–858
2. Orra K, Choudhury SK (2018) Mechanistic modelling for predicting cutting forces in machining considering effect of tool nose radius on chip formation and tool wear land. Int J Mech Sci 142–143:255–268
3. Heydarzadeh MS, Rezaei SM, Azizi N, Kamali E A (2018) Compensation of friction and force ripples in the estimation of cutting forces by neural networks. Measurement 114:354–364
4. Joardar H, Das NS, Sutradhar G, Singh S (2014) Application of response surface methodology for determining cutting force model in turning of LM6/SiCP metal matrix composite. Measurement 47: 452–464
5. Hanief M, Wani MF, Charoo MS (2017) Modeling and prediction of cutting forces during the turning of red brass (C23000) using ANN and regression analysis. Eng SciTechnol An Int J 20(3): 1220–1226
6. Cascón I, Sarasua JA (2015) Mechanistic model for prediction of cutting forces in turning of non-axisymmetric parts. Procedia CIRP 31:435–440
7. Dorlin T, Guillaume F, Costes JP (2015) Analysis and modeling of the contact radius effect on the cutting forces in cylindrical and face turning of Ti6Al4V titanium alloy. Procedia CIRP 31:185–190
8. Wyen C-F, Wegener K (2010) Influence of cutting edge radius on cutting forces in machining titanium. CIRP Ann 59(1):93–96
9. Rey PA, LeDref J, Senatore J, Landon Y (2016) Modelling of cutting forces in orbital drilling of titanium alloy Ti–6Al–4V. Int J Mach Tools Manuf 106:75–88
10. Ribeiro Filho SLM, Lauro CH, Bueno AHS, Brandão LC (2016) Influence cutting parameters on the surface quality and corrosion behavior of Ti–6Al–4V alloy in synthetic body environment (SBF) using response surface method. Measurement 88:223–237
11. Lauro CH, Ribeiro Filho SLM, Brandão LC, Davim JP (2016) Analysis of behaviour biocompatible titanium alloy (Ti-6Al-7Nb) in the micro-cutting. Measurement 93:529–540
12. Lauro CH, Brandão LC, Ribeiro Filho SLM, Davim JP (2018) Behaviour of a biocompatible titanium alloy during orthogonal micro-cutting employing green machining techniques. Int J Adv Manuf Technol 98:1573–1589. https://doi.org/10.1007/s00170-018-2352-8
13. Horváth R (2015) A new model for fine turning forces. Acta Polytechnica Hungarica 12(7):109–128
14. Lamikiz A, Lopez de Lacalle LN, Sanchez JA, Bravo U (2005) Calculation of the specific cutting coefficients and geometrical aspects in sculptured surface machining. Mach Sci Technol 9(3):411–436
15. Kienzle O, Victor H (1952) Die bestimmung von kräften und leistungen an spanenden werkzeugmaschinen. VDI-Z 94:299–305
16. Grądzka DS, Nejman M, Jemielniak K (2018) Relation between power and linear model of dynamic cutting coefficients, 11th CIRP conference on intelligent computation in manufacturing engineering, CIRP ICME '17. Procedia CIRP 67:274–277
17. Horváth R, Lukács J (2017) Application of a force model adapted for the precise turning of various metallic materials. Stroj Vestn-J Mech E 63(9):489–500
18. Meng Q, Arsecularatne JA, Mathew P (2000) Calculation of optimum cutting conditions for turning operations using a machining theory. Int J Mach Tool Manu 40:1709–1733
19. Boujelbene M (2018) Investigation and modelling of the tangential cutting force of the titanium alloy Ti-6Al-4V in the orthogonal turning process. 2nd International Conference on Materials Manufacturing and Design Engineering. Procedia Manuf 20:571–577
20. Khan MA, Mozammel Mia M, Dhar NR (2016) High-pressure coolant on flank and rake surfaces of tool in turning of Ti-6Al-4V: investigations on forces, temperature, and chips. Int J Adv Manuf Technol 90:5–8 1977–1991
21. Mia M, Khan MA, Dhar NR (2017) Study of surface roughness and cutting forces using ANN, RSM, and ANOVA in turning of Ti-6Al-4V under cryogenic jets applied at flank and rake faces of coated WC tool. Int J Adv Manuf Technol 93:1–4 975–991
22. Kobayashi E, Wang TJ, Doi H, Yoneyama T, Hamanaka H (1998) Mechanical properties and corrosion resistance of Ti-6Al-7Nb alloy dental castings. J Mater Sci Mater Med 9(10):567–574
23. Carou D, Rubio EM, Agustina B, Teti R (2017) Sustainable turning of the Ti-6Al-4V alloy at low feed rates: surface quality assessment. Procedia Manuf 8:769–774
24. Hertel M, Dix M, Putz M (2018) Analytic model of process forces for orthogonal turn-milling. Prod Eng:12/3–4, 491–500
25. Oliveira JA, Ribeiro FSLM, Lauro CH, Brandão LC (2017) Analysis of the micro turning process in the Ti-6Al-4V titanium alloy. Int J Adv Manuf Technol 92:4009–4016
26. Silva RB, Sales WF, Costa ES, Ezugwu EO, Bonney J, Silva MB, Machado AR (2017) Surface integrity and tool life when turning of Ti-6Al-4V with coolant applied by different methods. Int J Adv Manuf Technol 93(5–8):1893–1902
27. Mahapatro A (2015) Bio-functional nano-coatings on metallic biomaterials. Mater Sci Eng: C 55:227–251